AD-A039 858 HARVARD UNIV CAMBRIDGE MASS DIV OF ENGINEERING AND --ETC F/G 7/4
THE VISCOSITY AND STRUCTURAL RELAXATION RATE OF EVAPORATED AMOR--ETC(U)
MAY 77 R B STEPHENS N00014-77-C-0002

UNCLASSIFIED TR-1 NL

1 OF 1
AD A039 858

END

DATE FILMED
6-77

12

Office of Naval Research
Contract N00014-77-C-0002 NR-032-544

THE VISCOSITY AND STRUCTURAL RELAXATION RATE OF EVAPORATED AMORPHOUS SELENIUM

By

R. B. Stephens

Technical Report No. 1

May, 1977

Division of Engineering and Applied Physics
Harvard University • Cambridge, Massachusetts

Unclassified

SECURITY CLASSIFICATION OF THIS PAGE *(When Data Entered)*

REPORT DOCUMENTATION PAGE

READ INSTRUCTIONS BEFORE COMPLETING FORM

1. REPORT NUMBER: Technical Report No. 1
2. GOVT ACCESSION NO.
3. RECIPIENT'S CATALOG NUMBER
4. TITLE *(and Subtitle)*: THE VISCOSITY AND STRUCTURAL RELAXATION RATE OF EVAPORATED AMORPHOUS SELENIUM.
5. TYPE OF REPORT & PERIOD COVERED: TR-1
6. PERFORMING ORG. REPORT NUMBER
7. AUTHOR(s): R. B. Stephens
8. CONTRACT OR GRANT NUMBER(s): N00014-77-C-0002
9. PERFORMING ORGANIZATION NAME AND ADDRESS: Division of Engineering and Applied Physics, Harvard University, Cambridge, MA 02138
10. PROGRAM ELEMENT, PROJECT, TASK AREA & WORK UNIT NUMBERS
11. CONTROLLING OFFICE NAME AND ADDRESS
12. REPORT DATE: May 1977
13. NUMBER OF PAGES: 36
14. MONITORING AGENCY NAME & ADDRESS *(if different from Controlling Office)*
15. SECURITY CLASS. *(of this report)*: unclassified
15a. DECLASSIFICATION/DOWNGRADING SCHEDULE

16. DISTRIBUTION STATEMENT *(of this Report)*

This document has been approved for public release and sale; its distribution is unlimited. Reproduction in whole or in part is permitted by the U.S. Government.

17. DISTRIBUTION STATEMENT *(of the abstract entered in Block 20, if different from Report)*

NTIS White Section
DDC Buff Section
UNANNOUNCED
JUSTIFICATION
BY
DISTRIBUTION/AVAILABILITY CODES
DIST. AVAIL. and/or SPECIAL
A

18. SUPPLEMENTARY NOTES

19. KEY WORDS *(Continue on reverse side if necessary and identify by block number)*

Viscosity
Relaxation rate
Amorphous selenium
Heat capacity

20. ABSTRACT *(Continue on reverse side if necessary and identify by block number)*

For this study, thin film Se samples were vacuum deposited in order to produce a molecular structure significantly different from those of the previously studied melt-quenched samples. The structure differences should have been reflected in changes in their macroscopic properties.

We looked at the shear and volume viscosity, and heat capacity of configurationally equilibrated systems, and found no observable differences from melt-quenched samples; we took this as an indication that the selenium achieves configurational equilibrium rapidly even at relatively low temperatures

DD FORM 1 JAN 73 1473 EDITION OF 1 NOV 65 IS OBSOLETE

Unclassified

SECURITY CLASSIFICATION OF THIS PAGE *(When Data Entered)*

16375P EHH

and were able to measure the equilibration rate.

We have, however, produced non-equilibrium samples which have a much lower T_g (i.e., viscosity) than melt-quenched or annealed samples. We looked at the far infrared spectrum of these samples before and after equilibration and found no significant changes. Their T_g was too low to permit the handling necessary for a creep experiment.

Our viscosity data extend the previous data of Cukierman and Uhlmann, and Jenckel to lower temperatures. We find, in contrast to the higher temperature WLF type behavior, that the data show Arrhenius behavior between 25 and 35°C (~~2×10^{14} to 10^{11} poise~~); the slope is 130 kcal/mole. This low temperature Arrhenius-high temperature WLF behavior is similar to that observed by Macedo for B_2O_3.

~~We have also used~~ these measurements to determine stress and thermal relaxation rates as a function of temperature. They are not directly proportional to the equilibrium viscosity; the coefficient changes by a factor of 7 over the range 25 to 36°C. We take this to be the result of a temperature dependent equilibrium structure.

~~In addition~~, the relaxation to equilibrium is not a simple exponential decay. That has been observed many times previously; however, we have noticed that for this viscous relaxation data one does not need to invoke a spectrum of activation energies in order to fit the decay. The data can be simply described in terms of a relaxation rate, $1/\tau$, which is inversely proportional to the time dependent viscosity, η. [In other words, $1/\tau = a(1/\eta)$.] This simplification is not possible for the calorimetric relaxation data.

These results are consistent with the view that amorphous selenium is a mixture of 8 atom rings and polymeric chains which can readily interconvert and whose ratio is temperature dependent.

Office of Naval Research

Contract N00014-77-C-0002

NR-032-544

THE VISCOSITY AND STRUCTURAL RELAXATION RATE OF EVAPORATED AMORPHOUS SELENIUM

By

R. B. Stephens

Technical Report No. 1

May 1977

The research reported in this document was made possible through support extended the Division of Engineering and Applied Physics, Harvard University, by the Office of Naval Research, under Contract N00014-77-C-0002.

Divison of Engineering and Applied Physics

Harvard University · Cambridge, Massachusetts

I. INTRODUCTION

It has been thought for many years that amorphous selenium, by analogy to sulfur, is a molecular solid mixture of eight member rings and polymeric chains. Briegleib[1] and others[2,3] supported this hypothesis by demonstrating that, like sulfur, one fraction of amorphous selenium (a-Se) is much more soluble in cold CS_2 than another; presumably these correspond to the ring and chain fractions, respectively.[4] They found that, also like sulfur, the relative size of the two fractions can be manipulated by changing the temperature from which the melt is quenched. The different molecular structures produced by quenching from different temperatures have shown up in resistivity measurements[2] and in viscosity measurements both above[5] and below[6] T_g, and in T_g, the modulus, and density,[6] but the variations were rather small,[7] and no one has tried to measure the relative stability of these different structures. The objective of this work was to produce selenium in non-equilibrium states whose composition could be probed by the manner in which they relaxed toward equilibrium. Samples were produced by vacuum evaporation. It was expected that this procedure would skew the molecular structure toward smaller chains and more rings, and that the skewing would be much larger than can be achieved through melt-quenching.[8] Thus, the effects of molecular structure should be considerably larger than in earlier experiments - in fact, large enough to measure the kinetics of structural equilibration. Toward that end, we measured the viscosity and heat capacity of these samples as a function of temperature, and also their far infrared (FIR) transmission spectra.

II. EXPERIMENTAL DETAILS

The samples were produced from 5-9's pure Se pellets.[9] The pellets were premelted and outgassed in vacuum (typically 8×10^{-7} mmHg), and then evaporated

onto a temperature controlled substrate - a NaCℓ coated glass slide. The samples were ∿100μm thick and produced in 20 min. They were floated off the glass in water.

For viscosity measurements, the substrate was held at 20°C, and masked to produce a specimen as shown in Fig. 1a. This was clamped into one arm of a balance beam (Fig. 1b), 40 grams were hung from the other arm, and the resulting creep was monitored by a linear voltage displacement transformer (LVDT)[10] which surrounded an iron core built into the weighted arm of the balance. The narrow part of the sample was surrounded by a slot in a termperature controlled aluminum block. Thermal contact was maintained by filling the slot with oil. The apparatus was operated in a temperature controlled box set at ∿4°C to eliminate expansion or contraction of the various components of the balance beam, and also to eliminate contributions to the creep by the end tabs of the sample. The instrument was calibrated by shifting the LVDT a measured distance with a calibrated screw. This screw was also connected to a low speed motor which periodically lowered the transformer to prevent the recorder pen from going off scale.

The film cross sections were $\sim 2\times10^{-3}$ cm^2, so that we were imposing a stress of $\sim 10^7$ dynes/cm^2. According to the previous work by Jenckel,[11] this is well within the limits of stress for Newtonian flow.

The heat capacities were measured in a Perkin-Elmer Differential Scanning Calorimeter (DSC-II). The samples for this were prepared as described in the first paragraph of this section except that no evaporation mask was used in this case. The substrate was held at temperatures from 14°C (cooling water) to -196°C (liquid nitrogen). The samples were floated off the substrate in ice water. Then they were dried, broken up, sealed inside aluminum planchettes, and stored on dry ice until they were used.

The infrared spectra were obtained from a Digilab Fourier transform spectrometer at MIT. In this case, the films had to be evaporated through a screen so that the surface would be uneven enough to average out interference effects. The screen was made of parallel 1 mil wires spaced by ∿1 mil, and it was moved twice during evaporation to randomize the surface fluctuations. In order to preserve the evaporated structure, the substrate was kept at -57°C (using a mixture of dry ice and acetone), and the samples then handled as for the calorimeter. The spectra were taken in times much shorter than those needed for measurable structural relaxation.

III. VISCOSITY RESULTS

The procedure for making the measurements was as follows: The creep rate was monitored at constant temperature until steady state was achieved. Then the temperature was changed very quickly (compared to the equilibration rate) to a new temperature, held there, and the creep rate was monitored until a new steady state creep was reached. The sample was under a constant stress at all times.

With this procedure, four independent parameters can be obtained: 1) the equilibrium viscosity as a function of temperature; 2) the isostructural viscosity activation energy; 3) the relaxation rate; 4) the analytical form of the relaxation.

The equilibrium viscosity is shown in Fig. 2. The solid line is a fit to the previous data on melt-quenched samples; Jenckel,[11] who did creep measurements, and Cukierman and Uhlmann,[12] who did beam bending measurements. Note that in the region of overlap, the data are virtually identical. It is clear from our additional low temperature data that the analytical form of the temperature dependence of the viscosity is very different from that used by Cukierman and Uhlmann in the higher temperature range. Instead of the WLF type curve, which

has a slope which increases with decreasing temperature [$\eta \propto \exp a/(T-T_o)$], and which fits the data well for T>35°C; the data for T<35°C has the form of a simple exponential with a slope of 127.9 kcal/mole and a prefactor of -182.6. This change to Arrhenius behavior is similar to the behavior exhibited by B_2O_3 in the same viscosity region.[13]

The second parameter I have called the isostructural viscosity activation energy. In the free volume model, the isostructural viscosity is equivalent to the volume viscosity and is a measure of the ease with which the free volume can be re-equilibrated after a rapid temperature change. It is obtained by noting the change in viscosity of the sample after a very rapid change in temperature, and so one is measuring the temperature dependence of the viscosity of a fixed structure (that is the structure which was in equilibrium at the starting temperature). The rapid nature of this measurement introduces considerable scatter in the results, but one can see in Fig. 3 that the activation energy averages ∿77 kcal/mole. This is ∿50kcal/mole less than the equilibrium viscosity activation energy; the difference presumably being the activation energy required to re-equilibrate the molecular structure after a temperature change. One might expect the equilibration to involve breaking Se-Se bonds in order to change the average Se chain length, or ring concentration.[14] It is gratifying to note that our measured value (∿50 kcal/mole) is reasonably close to the energy of such a bond (44-50 kcal/mole).[15]

After a temperature change, the relaxation of the creep rate toward its equilibrium value is clearly not a simple exponential decay (Fig. 4). That is not unusual; simple relaxations are never observed in complicated systems such as polymers.[16] However, for an adequate fit, it is not necessary to invoke a spectrum of relaxation times, as is customary in such cases. One can achieve a good fit with a much simpler expression (Fig. 4) by supposing that the relaxation rate, $1/\tau$, is proportional to the creep rate, R. Thus, a sample initially in a

non-equilibrium state, will relax toward equilibrium in the following manner:

$$R(t) = 1/\tau(R)[R(t)-R_e] \qquad (1)$$

where R_e is the steady state creep rate, and $1/\tau(R)$ is the instantaneous relaxation rate. The simplest assumption (which turns out to be not quite true) is that $1/\tau(R) = aR$. Then one has:

$$\dot{R} = -aR(R-R_e). \qquad (2)$$

The solution to this differential equation is relatively simple:

$$R(t) = R_i R_e / [R_i - (R_i-R_e)\exp(-aR_e t)] \qquad (3)$$

where $R(t)$ = the time dependent creep rate, R_i = the initial creep rate, R_e = the equilibrium creep rate, and a = the relaxation rate/creep rate. We have measured the time dependence of the creep rate when approaching equilibrium from both above and below the equilibrium temperature (see Fig. 5) and can fit the data well using R_i, R_f, and a as free parameters. Plotting them as functions of temperature (Figs. 2,3, and 6) we found smooth curves, indicating that our fit was not a fortuitous result of the uncertainties in our data. We also found that a had a very definite temperature dependence (Fig. 6); it changes by more than a factor of 5 over our experimental range. The significance of this variation in a is uncertain. From a very simple point of view the relaxation time is determined by the number of molecular displacements needed to equilibrate a structure divided by the rate of these displacements, while the viscosity is determined primarily by the rate of molecular displacements. Therefore the ratio, a, is simply proportional to the number of displacements needed for equilibration, and should be determined by the structure of the molecule and its environment - smaller molecules equilibrating more rapidly than larger ones and large molecules surrounded by small ones relaxing more rapidly than those entangled in many other large ones. For both reasons the observed temperature dependence of a suggests that as one lowers the temperature, the equilibrium structure of amorphous selenium changes in favor of rings at the expense of long chains.

IV. INFRARED SPECTRA RESULTS

The far infrared spectrum is shown in Fig. 7. As stated in the experimental section, the films were evaporated onto a cold substrate and kept cold and dark until use to preserve any structural differences. After several scans, they were heated in water to 50 to 70°C for 15 min. This is well above T_g, and from the creep data, considerably longer than needed for equilibration. The annealed sample's spectrum is virtually the same as the as-prepared sample's.

The invariance of Se's far infrared optical spectra has been demonstrated previously with samples quenched from different melt temperatures.[17] The Raman spectrum has been shown also to be independent of sample preparation techniques for both melt-quenched and evaporated samples.[18] Taken together, these results strongly suggest that the molecules making up amorphous Se interact too strongly to be able to identify an absorption line with a particular species as had been suggested for Se.[19]

V. HEAT CAPACITY RESULTS

Another way to investigate relaxation rates in selenium is to look at its heat capacity as a function of thermal history in the neighborhood of the glass transition temperature, T_g.[20,21] A typical heat capacity scan for Se at T_g is shown in Fig. 8. At 2.5°/min. the heat capacity increases by 50% over a range of only $\sim$10°K at 310°K. In spite of this discontinuous appearance, the glass transition is, of course, not a thermodynamic transition and its presence does not imply a discontinuity in a material's equilibrium properties.[22] One can demonstrate that the step is a direct consequence of a glass's temperature dependent structural relaxation rates.[21,23] We have devised a simple iterative equation which keeps track of the excess enthalpy contained in a sample as it is scanned in temperature:

$$\Delta H_n = \frac{C_{config}}{2}\Delta T + \left\{\frac{C_{config}}{2}\Delta T + \Delta H_{n-1}\right\} \exp\left[-\Delta t/\tau(t)\right] \qquad (4)$$

where ΔH_n is the excess enthalpy at the end of a step of time Δt and the temperature change ΔT. C_{config} is the heat capacity associated with the structural degrees of freedom; these degrees of freedom have a relaxation time $\tau(T)$. Depending on one's sophistication, the structural relaxation time can be simply described by:[24]

$$\tau = \exp(a + b/(T-T_o)] \qquad (5)$$

or one can improve the model by adding an intermediate step to account for the finite relaxation rate of τ, as discussed in the viscosity section.

Then the heat removed from the sample at each step is given by the change in the excess enthalpy ($\Delta H_n - \Delta H_{n-1}$) plus the change in the equilibrium enthalpy $C_{equil}\Delta T$; the observed heat capacity is:

$$C_{obs} = C_{equil} + (\Delta H_{n-1} - \Delta H_n)/\Delta T \qquad (6)$$

If one measures T_g as a function of scan rate (we defined T_g as the temperature at which we measured half of the structural heat capacity), one can invert this process and, by trial and error, determine the relaxation time as a function of temperature. Using the experimental data in Table I, we got fits of the heat capacity curves as shown by the dashed line in Fig. 8 and the relaxation times indicated by solid dots in Fig. 9. By reducing the isostructural activation energy to 55.6 kcal/mole, we could slightly improve the match with the experimental curve (the dotted line in Fig. 8). For a more detailed agreement one can use the equations formulated by De Bolt *et al.*[21] which make use of a spectrum of relaxation times. We have not tried to use their equations to calculate relaxation times, as our simple equations produce reasonable fits to experiment. Note that even though the scan rates spanned 0.3 to 20°/min., the range of the data was limited to about 10°C by the very rapid change of τ with temperature.

Table I

Selenium glass transition temperature, T_g, vs. scan rate. T_g is taken to be the temperature at which the observed heat capacity is halfway between the extrapolated glass and liquid values. The relaxation time at those temperatures was determined by numerically simulating the heat capacity as decribed in the heat capacity section, and adjusting $\tau(T)$ until the calculated T_g matched experimental T_g to $\leq$ .2K, then calculating $\tau(T_g)$.

Scan rate (K/min)	T_g (K)	$\tau(Tg)$(min)
20	314.6	.14
10	313.1	.25
5	311.4	.69
2.5	310.1	1.0
1.25	309.2	2.3
.625	307.8	4.4
.3125	307.0	6.8

One can extend the data to lower temperatures using the procedure outlined in Fig. 10. Starting at some temperature $T_I > T_g$, with the sample in thermal equilibrium, one cools to $T_A < T_g$ and holds it there for a time t_A. As it cooled below T_g, the molecular structure was nearly immobilized, so that when one reached T_A, the structure was not in equilibrium and had an excess enthalpy which, during the annealing time, slowly relaxes out. The heat is being released so slowly that it is very hard to detect. However, when the sample is warmed above T_g, it returns to thermal equilibrium, and that heat has to be replaced. As a result, an endothermic relaxation peak is observed at T_g whose area is equal to the energy lost during the annealing. When this area is recorded (minus the area of the small peak observed for $t_A = 0$) as a function of t_A, one can determine a relaxation curve for T_A. The low temperature limit on this method is determined solely by the experimenter's patience. In our case, we went down to 294°K by annealing for periods up to 3 days. The curves are shown in Fig. 12; they have been normalized by the enthalpy the sample would lose if it had completely equilibrated at T_A.[25] The curves are clearly not the result of a single relaxation time; the form of that relaxation is indicated by the dotted line in Fig. 10. The curves even look smeared out compared to the form resulting from the relaxation proposed in the viscosity section (the dashed line in Fig. 12). It was calculated for $T_A = 300°K$; the initial relaxation rate was estimated from the data on Fig. 10. Clearly these curves reflect a wide spectrum of relaxation times; if one models the curve with a Gaussian in the log of the relaxation times, one finds a good match for a half width of .7 (i.e., it spans a factor of 5 in the relaxation times).

We have taken the 50% relaxation times from these curves and plotted them (the x's) with the other relaxation times in Fig. 9. The agreement is very satisfying.

In a final set of samples, we used measurements of T_g to look for non-equilibrium molecular structures. Since we produced our samples by vacuum evaporation, the concentration of shorter chains and rings should be considerably enhanced. However, if the substrates were too warm, the samples could have annealed to an equilibrium structure before any measurements were made. Therefore we tried a series of evaporations onto cooled substrates. Since such non-equilibrium structures might be very active, they were handled with great caution; they were removed from the substrate in ice water, stored in dry ice, and, as far as practicable, were not exposed to light. The resulting heat capacities are shown in Fig. 12; one can see two significant differences from the curve for the annealed sample (the dashed line): 1) The glass transition temperature is considerably lower for the samples from the colder substrates. For the selenium laid down on the coldest substrate it is reduced about 10°K to 305°K. In Fig. 12, we see that the temperature corresponds to a τ of $\sim$30 min. in equilibrated Se, whereas T_g occurs at a τ of $\sim$.15 min. The viscosity in this sample is $\sim$200 × lower than in equilibrated samples. 2) Immediately after the relaxation peak is a broad exothermic peak which is never seen in quenched samples annealed at any temperature. Since it partly overlies the relaxation peak, it is impossible to measure the energy involved.

If the sample is either exposed to light (at T=273°K), or thermally annealed (see Fig. 13) T_g increases in temperature and the exothermic peak decreases in area; after a sufficient amount of annealing (one scan all the way through the exothermic peak, to 350°K is sufficient), the glass transition looks identical to that of an equilibrated sample made by any other method.

Clearly we are producing, and freezing in, a molecular configuration of low viscosity and some photoactivity. It is unstable and reduces exothermically to the equilibrium configuration at a rate limited only by the speed of molecular

movements. It may be that this is primarily a ring glass. However, as noted in the IR spectra section, there was no significant difference in absorption between freshly evaporated and equilibrated samples. If that spectrum is indicative of the molecular species present, then it must be concluded that we have not increased the concentration of the rings; we have only produced a glass consisting of relatively short and/or poorly packed chains.

In any case, the nature of the relaxation of this structure into the equilibrium structure could be very informative if the experimental difficulties of handling it can be surmounted.

VI. DISCUSSION

The FIR absorption spectra showed only that it is not a fruitful technique to use as a probe of the molecular structure of condensed Se. Presumably the molecules interact too strongly to consider them as independent rings and chains with known vibrational modes. Recently Gorman and Solin[18] have claimed some success with a FIR Ramam setup; using the polarized and depolarized Raman spectrum together, they can single out a ring mode at 112 cm^{-1}. It might be fruitful to pursue that method further to see if that mode's relative intensity is a function of sample preparation technique or annealing time.

Our other experiments cannot elucidate the exact molecular composition of selenium, but they do reveal some interesting behavior which is consistent with an amorphous selenium consisting of a mixture of rings and chains. Clearly, from our heat capacity data, an evaporated sample initially has a structure very different from that of a melt-quenched or annealed sample. The evaporated sample had a viscosity at least 200× lower than the annealed samples. Since the viscosity scales faster than linearly with chain length,[26] that corresponds

to a drastic reduction in polymerization by a factor of 5 to a chain length of 10^5 atoms (if one takes an estimated equilibrium chain length[27] of 10^6). Therefore, these samples consist of shorter chains (and/or a higher concentration of rings). In spite of this structural difference, it appears that these samples readily anneal to an equilibrium state indistinguishable from equilibrated melt-quenched samples at temperatures as low as 25°C (about 20° below T_g). It can only be concluded that one anneals to a unique equilibrium state, and that, therefore, the molecular species can readily interconvert during annealing.

In addition, the observations (1) that the activation energy for the equilibrium viscosity is larger than that for the isostructural viscosity by about the strength of a Se-Se bond and (2) that the ratio of the relaxation time to viscosity is not a constant, suggests that the molecular structure is a function of temperature, and that the relaxation observed is primarily a result of the molecular species interconverting as they relax to their equilibrium concentrations.

Finally, since there appears to be no discontinuity in the elastic properties of this equilibrium state, one can rule out a sharp ring-chain transition analogous to that in sulfur above 25°C.[28] Rather, the smooth decrease in a with decreasing T suggests a gradual increase in ring concentrations as suggested previously.[29]

The form of the relaxation proposed here is quite successful at modeling the viscous relaxation, and relaxation times calculated independently from creep rate and T_g data agree reasonably well. In addition, it reproduces the general behavior of the heat capacity curves and thermal relaxation curves better than a simple exponential relaxation. However, in detail the experimental and predicted heat capacity curves do not match very well at all;

it is clear that there exist a wide range of relaxation times for the thermal relaxations, which are not apparent in the viscous relaxations.

This behavior is qualitatively consistent with a ring-chain model of selenium. It is reasonable to suppose that rings and chains have different relaxation rates and thermal relaxation measurements would show an appropriately weighted mixture of the two rates. However, it is only the long molecules which determine the viscosity and so the viscous relaxation measurements would show only the single time constant characteristic of long chains.

ACKNOWLEDGMENTS

The author is grateful to Professor David Turnbull for many helpful discussions during the course of this work. Thanks are due to Professor Marc Kastner in the MIT Physics Department and the MIT Center for Materials Science and Engineering, for the use of their Fourier Transform Spectrometer. This research was supported in part by the Office of Naval Research under contract N00014-77-C-0002 and by the Division of Engineering and Applied Physics, Harvard University. Also, use was made of facilities provided by the Advanced Research Projects Agency and the National Science Foundation.

*Present Address: Exxon Research and Engineering Co., P.O. Box 45, Linden, New Jersey 07036.

References

1. G. Brieglieb, Z. Phys. Chem., A144, 321-339; 339-358 (1929).

2. E. Grochowski, W. Brenner, J. Crystal Growth 13-14, 843 (1972).

3. M.C. Coughlin, B. Wunderlich, J. Poly. Sci. 11, 1735 (1973).

4. Selenium's photosensitivity apparently makes this a very difficult experiment to reproduce. Private communication, R.C. Keezer.

5. A. Eisenberg, A.V. Tobolsky, J. Poly. Sci. 61, 483-495 (1962).

6. L.J. Graham and R. Chang, J. Appl. Phys. 36, 2983-2986 (1965).

7. In fact there were no differences observed in the far infrared spectrum of selenium samples quenched from different temperatures; see R.C. Keezer, G. Lucovsky, R.M. Martin, Bull. Am. Phys. Soc. 20, 323 (1975). One can produce larger differences by chemically controlling the lengths of the Se chains with iodine or chlorine: see S. Hamada, T. Sata, T. Shira, Bull. Chem. Soc. Jap. 41, 135-139 (1968); A. Eisenberg, L. Teter, J. Am. Chem. Soc. 87, 2108-2113 (1965); R.C. Keezer, M.W. Bailey, Mat. Res. Bull. 2, 185-192 (1967).

8. This idea is by analogy to the behavior of sulfur. At 500°C, S liquid is predominantly long chains but S vapor is almost exclusively S_8 rings; see H. Rau, J.R.N. Kutty, J.R.F. Guedes de Carvallo, J. Chem. Thermodynamics 5, 833 (1973). If Se behaves similarly and its vapor can be condensed without repolymerization, the resulting film will have a very low molecular weight compared to the molecular weight of Se melts which do not change very much as a function of temperature: see Ref. 6, Fig. 9.

9. Ceracpur, Menominee Falls, Wisc.

10. Supplier: Shaevitz Engineering, Pennsauken, N.J.; SCM series, model SC I 025, #407.

11. E. Jenckel, Kolloid Zeit. 84, 266 (1938).

12. M. Cukierman and D.R. Uhlmann, J. Non. Cryst. Sol. 12, 199 (1973).

13. P.B. Macedo and A. Napolitano, J. Chem. Phys. 49, 1887 (1968).

14. A. Eisenberg, A.V. Tobolsky, J. Poly. Sci. 46, 19 (1960); A. Eisenberg, Poly. Lett. 1, 33 (1963).

15. L. Brewer, "Electronic Structure and Alloy Chemistry of Transition Elements", P.A. Beck, ed. (Interscience, New York 1963), p. 222; L. Pauling, "The Nature of the Chemical Bond", 3rd ed. (Cornell Press, Ithaca, N.Y. 1960). That agreement may be only coincidental, as one observes volume viscosity activation energies between 1/3 and 2/3 of that for the equilibrium viscosity (the ratio for Se is 2/3) in systems for which bond interchange is clearly not a contributing factor. See M. Goldstein, J. Chem. Phys. 64, 4767 (1976); R.S. Marvin and J.E. McKinney, "Physical Acoustics", Vol. IIB, W.P. Mason, ed. (Academic Press, New York 1965), p. 181; N. Hira, H. Eyring, J. Poly. Sci. 37, 51 (1959).

16. G.C. Berry, T.G. Fox, Adv. Polymer Sci. 5, 261 (1968).

17. R.C. Keezer, G. Lucovsky, R.M. Martin, Bull. Am. Phys. Soc. 20, 323 (1975).

18. J.E. Smith, Jr., M.H. Brodsky, R.J. Gambino, Bull. Am. Phys. Soc. 17, 336 (1972). Gorman and Solin claim to see some evidence of annealing on their FIR Raman spectra of evaporated Se films; see M. Gorman, S.A. Solin, Sol. State Commun. 18, 1401 (1976).

19. G. Lucovsky, Mat. Res. Bull. 4, 505 (1969).

20. J. Cornet, D. Rossier, Proceedings of the Fifth International Conference on Amorphous and Liquid Semiconductors, ed. J. Stuke and W. Brenig (London: Taylor and Francis, 1974), p. 267; G.C. Das, M.B. Bever, D.R. Uhlmann, J. Non. Cryst. Sol. 7 251 (1972); H. Gobrecht, G. Willers, D. Wobig, J. Phys. Chem. Sol. 31, 2145 (1970); C.T. Moynihan, A.J. Easteal, J. Wilder, J. Tucker, J. Phys. Chem. 78, 2673 (1974). There exist many articles which deal with relaxation processes in other materials -- primarily polymers. For a review see ref. 16.

21. M.A. DeBolt, A.J. Easteal, P.B. Macedo, C.T. Moynihan, J. Am. Ceram. Soc. 59, 16 (1976).

22. There may be such a discontinuity, but it would be directly observable only at infinitely slow cooling rate. For a discussion, see C.A. Angell, K.J. Rao, J. Chem. Phys. 57, 470 (1972).

23. S.M. Wolpert, A. Weitz, B. Wunderlich, J. Poly. Sci. A2 9, 1887 (1971).

24. These equations will fit in an HP-25 for this form of τ and $T_o = 0$ but the calculated relaxation times will be lower by $\sim$2x than the model with a finite relaxation rate for τ, and the transition will be considerably sharper.

25. That is the hatched area in Fig. 12; the energy is calculated by integrating the difference between the extrapolated liquid heat capacity and the $t_A = 0$ heat capacity down to T_A.

26. The exponent is 3.4 for chains longer than 200-400 atoms; see Berry and Fox, ref. 16.

27. That number was estimated for 300°K using Fig. 4 of A. Eisenberg and A.V. Tobolsky, J. Poly. Sci. 46, 19 (1960).

28. It had been placed at 77°C by Eisenberg and Tobolsky, ref. 27, and at 30°C by H. Gobrecht, G. Willers, D. Wobig, J. Phys. Chem. Solids 31, 2145 (1970).

29. R.B. Stephens, J. Non. Cryst. Sol. 20, 75 (1976); see Fig. 3

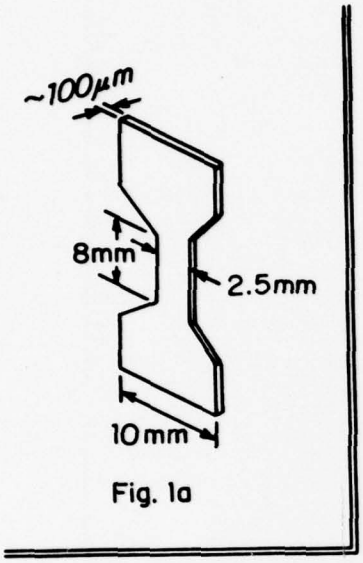

Fig. 1a

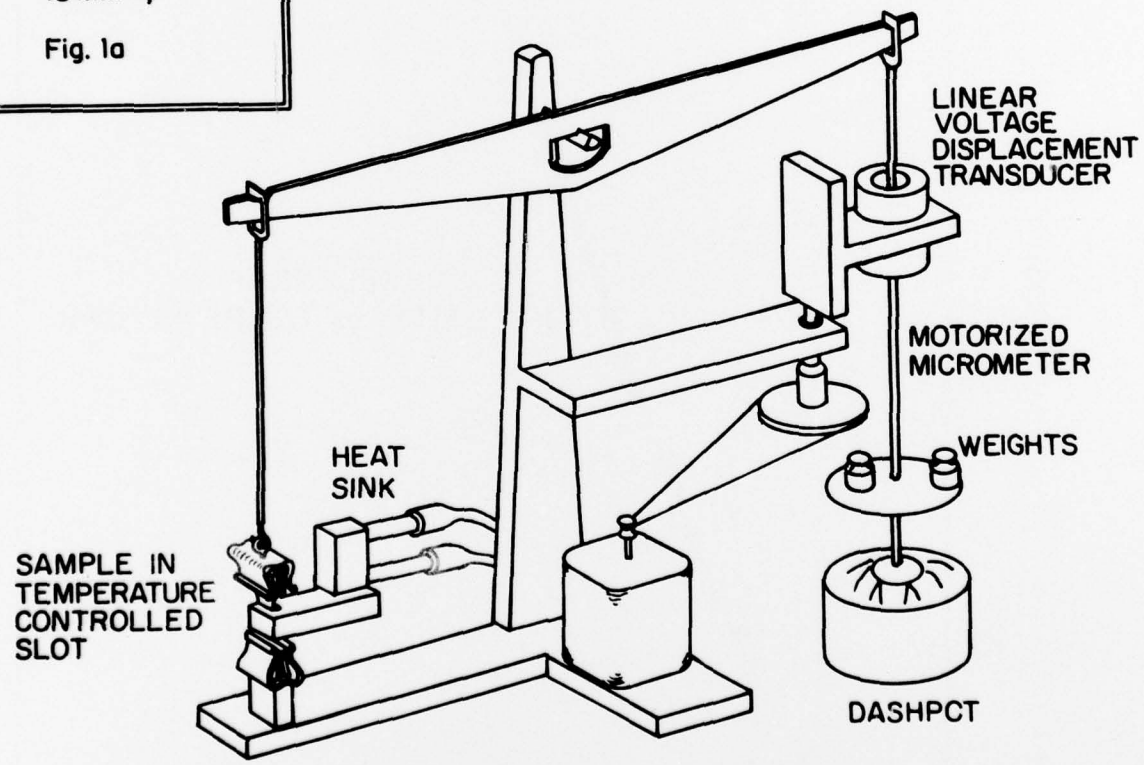

Fig 1b

Schematic drawing of a) a selenium creep sample and b) a balance modified for measuring creep. The sample is clamped on the left hand side of the balance. The narrow part is inserted in an oil filled slot in a temperature controlled Aℓ block. From the right hand side hangs a dashpot to damp vibrations, a tray for weights, usually 40 g, and an iron slug which is surrounded by a linear voltage displacement transducer attached to the frame. The transducer is mounted on a motor drive translation stage so it can be periodically repositioned when its output drives the recorder pen offscale.

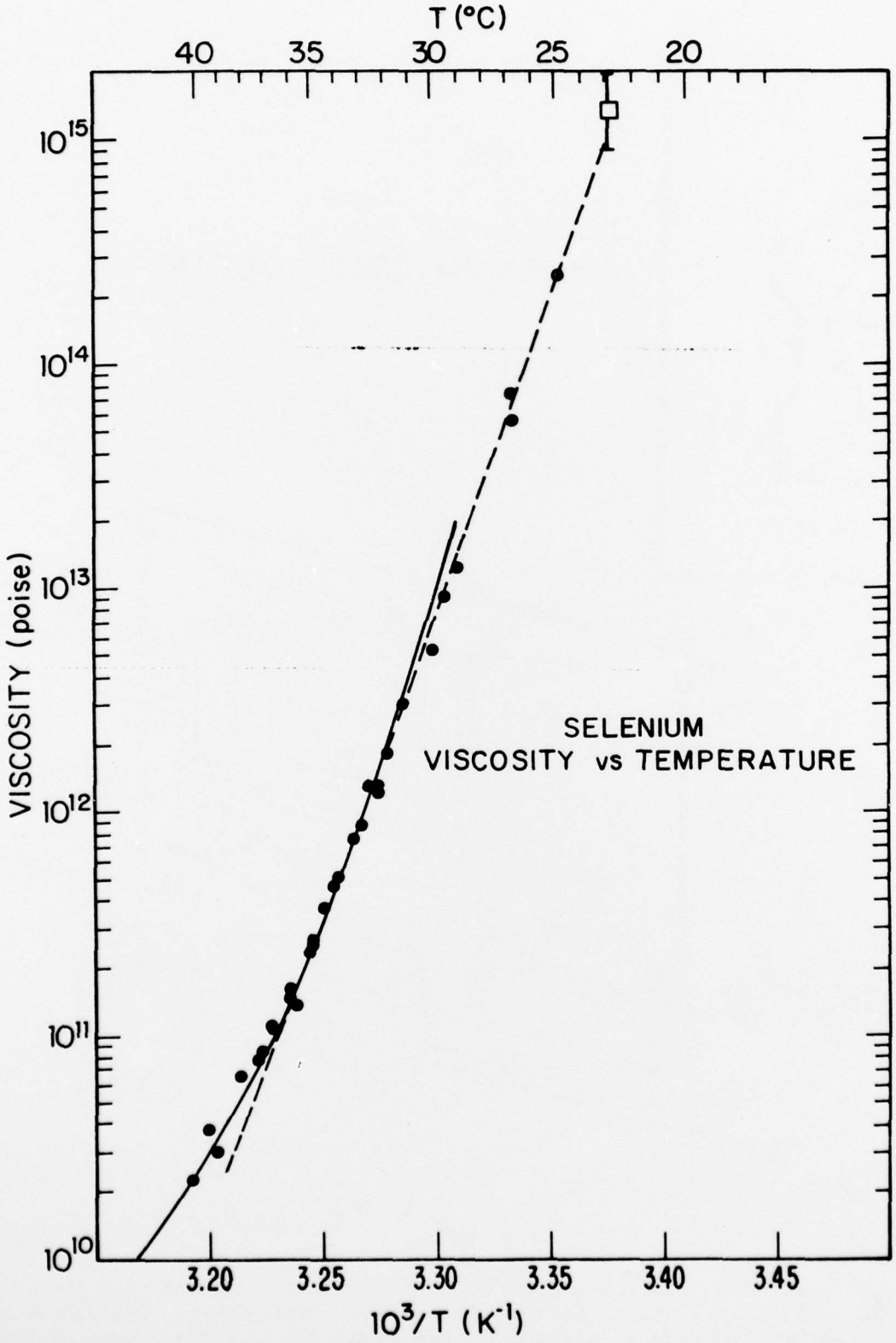

FIGURE 2: Selenium viscosity vs. temperature. The solid circles are from this work. The solid line is a fit to previous data by Cukierman and Uhlmann (a beam bending experiment),[12] and Henckel (a creep experiment),[11] the ⊓ covers the range of data by Grahan and Chang.[6] The dashed line is a fit to all of the data below 320°K, and has a slope of 127.9 kcal/mole and a prefactor of -182.6.

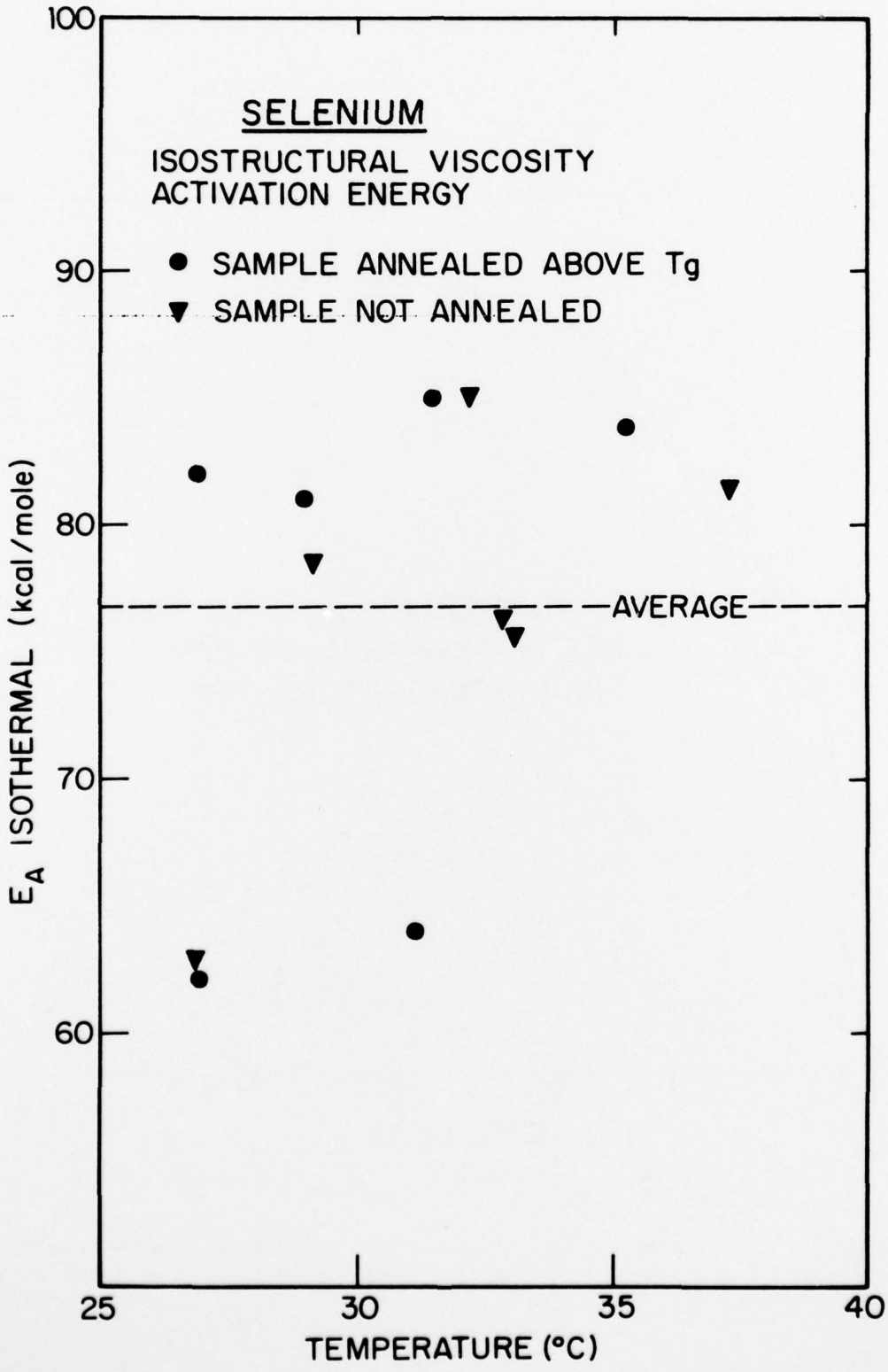

FIGURE 3: Selenium isostructural viscosity activation energy. Calculated from the change in a sample's viscosity after a rapid change in temperature. See text for a discussion of its significance.

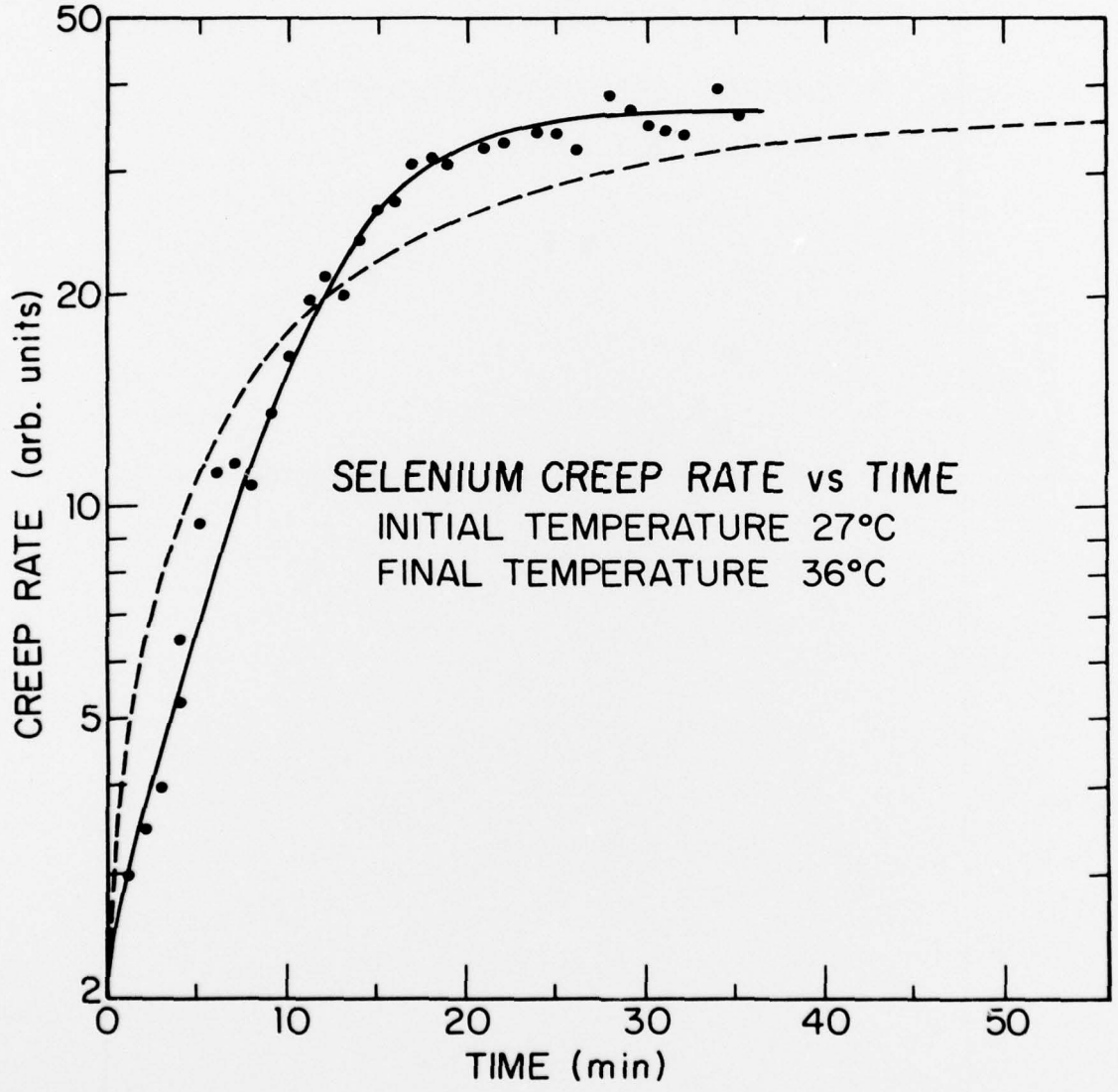

FIGURE 4: Selenium creep rate vs. time after a rapid temperature change from 27 to 36°C. The dashed line is a fit using an exponential decay, the solid line is a fit using Eq. (3). Both are three parameter fits.

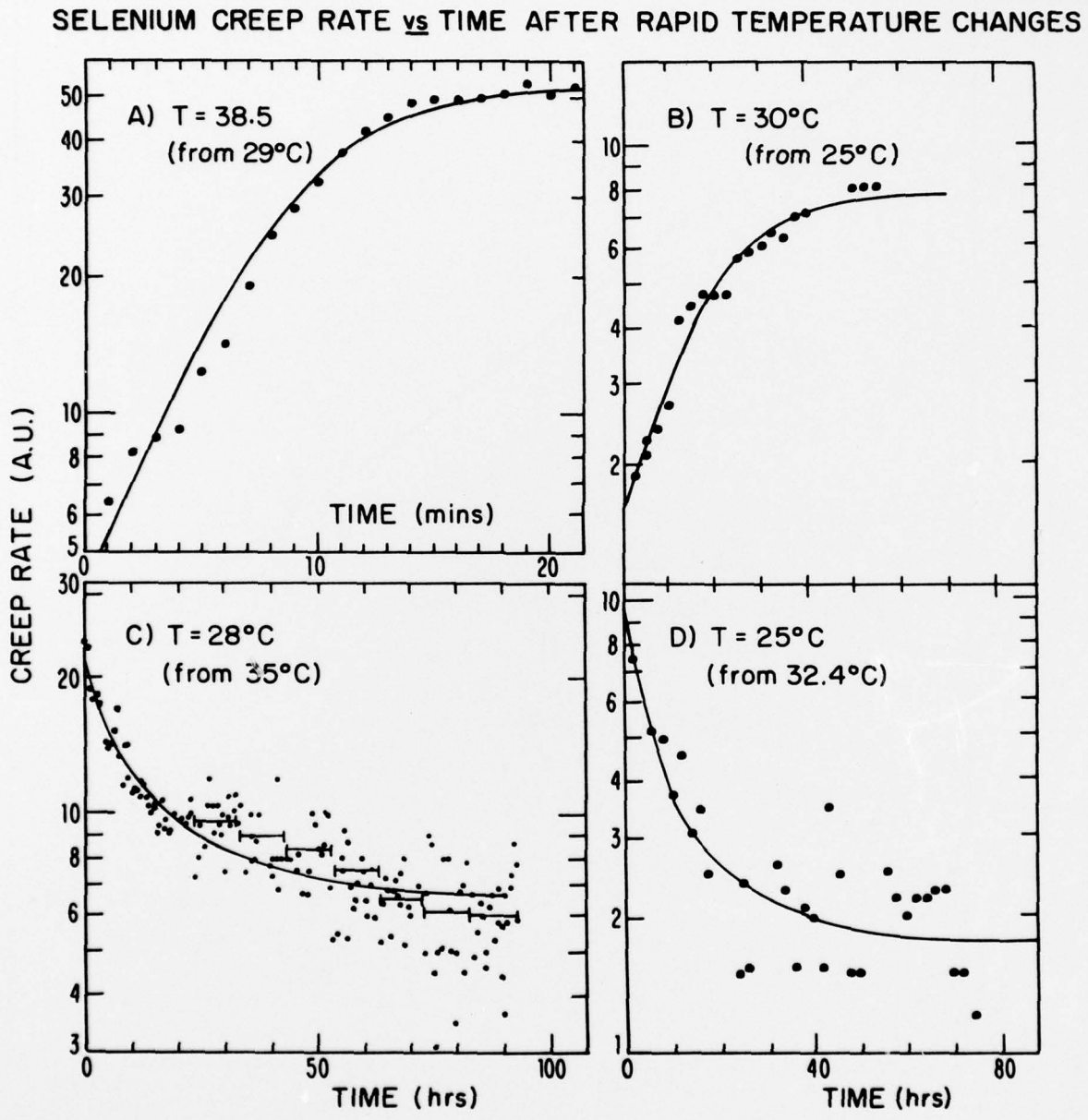

FIGURE 5: Selenium creep rate vs. time after rapid temperature changes a) from 29 to 38.5°C, b) from 25 to 30°C, c) from 35 to 28°C, and d) from 32.4 to 25°C. The solid lines are three parameter fits to the data using Eq. (3).

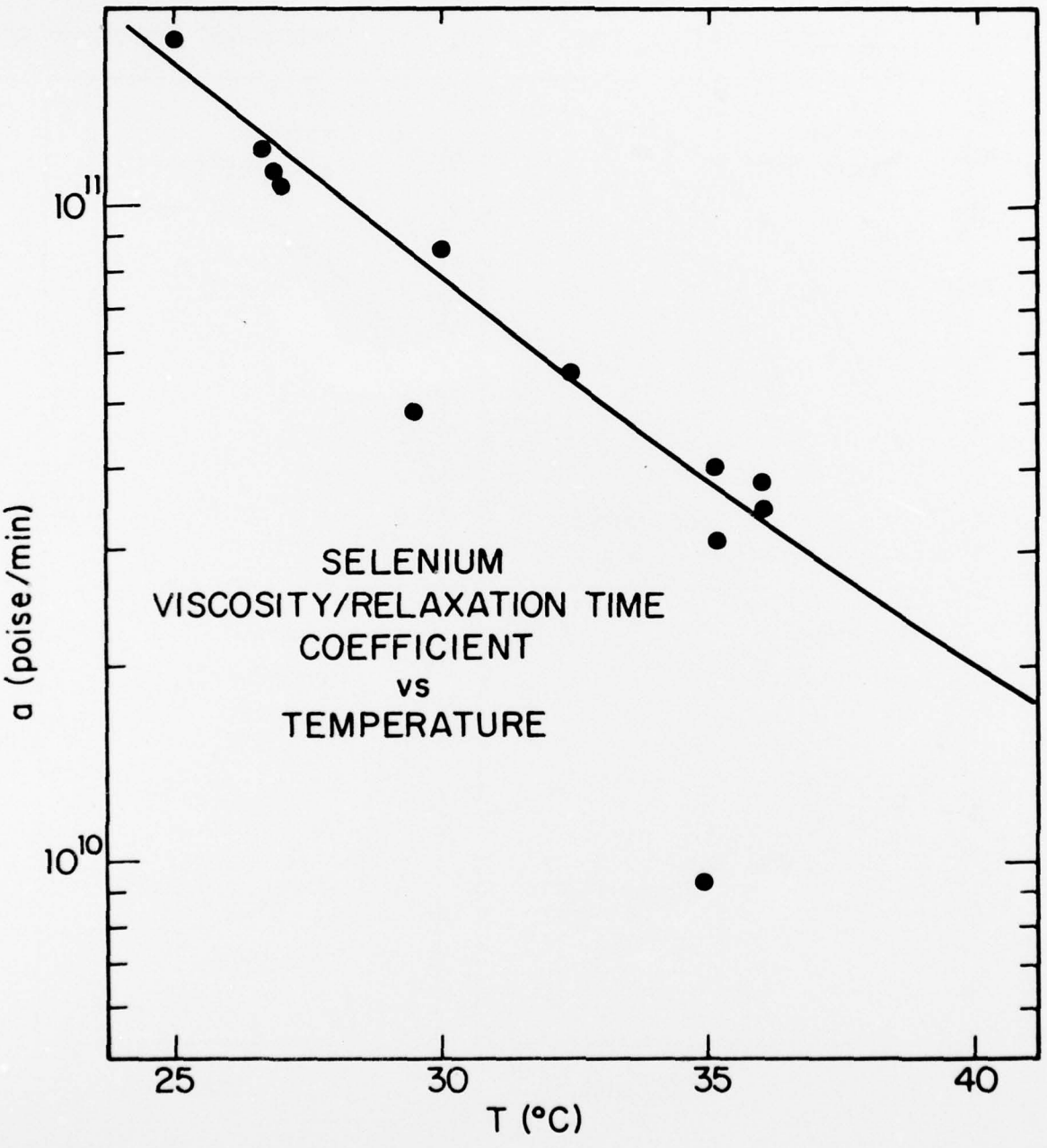

FIGURE 6: Selenium viscosity/relaxation time coefficient determined by fits to data as shown in Fig. 5. The data are ploteed as a function of the final sample temperature.

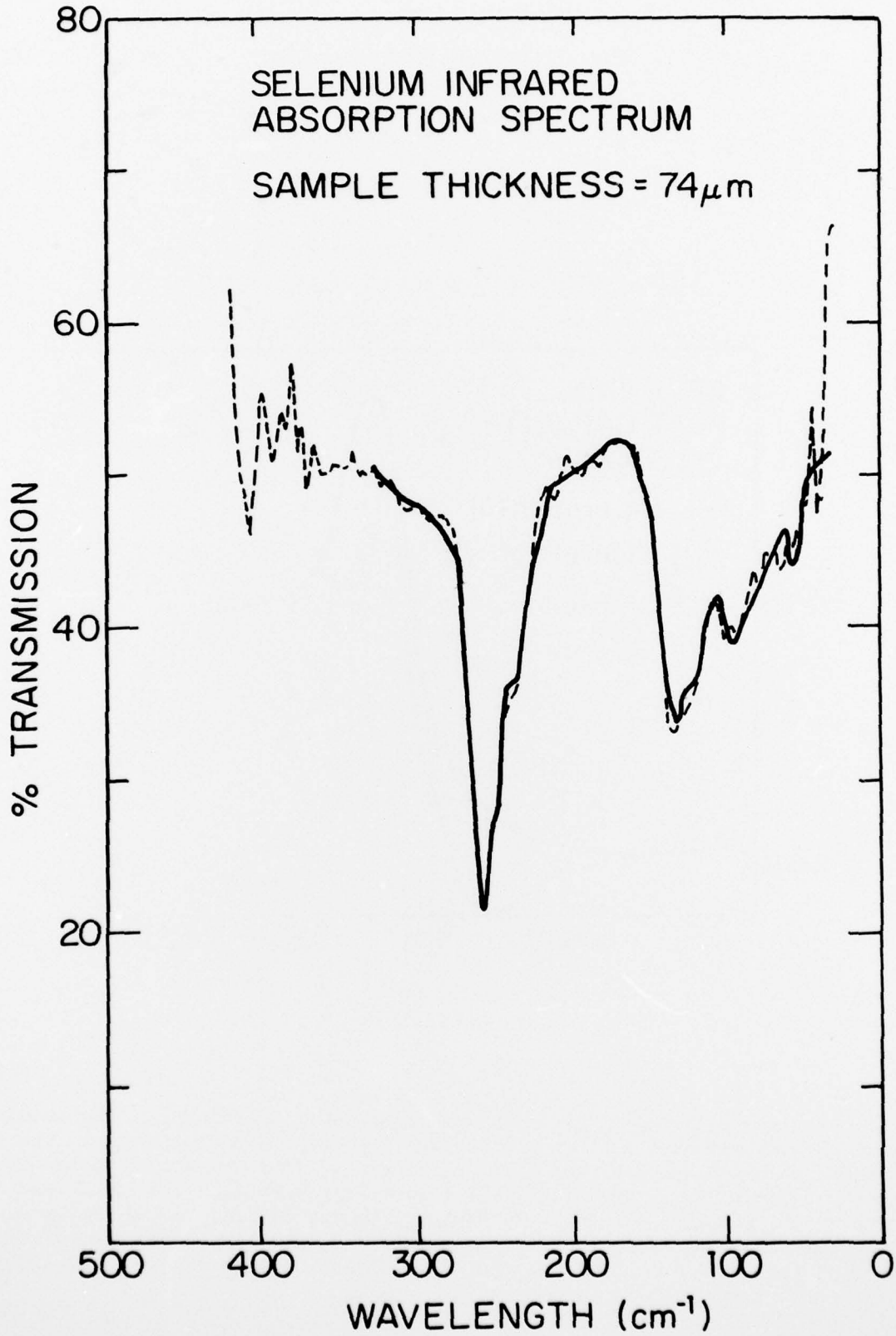

FIGURE 7: Far infrared absorption spectrum of selenium. The spectrum of the as prepared sample is indicated by a solid line, the spectrum of the annealed sample is indicated by a dashed line. There is no significant difference between the two curves.

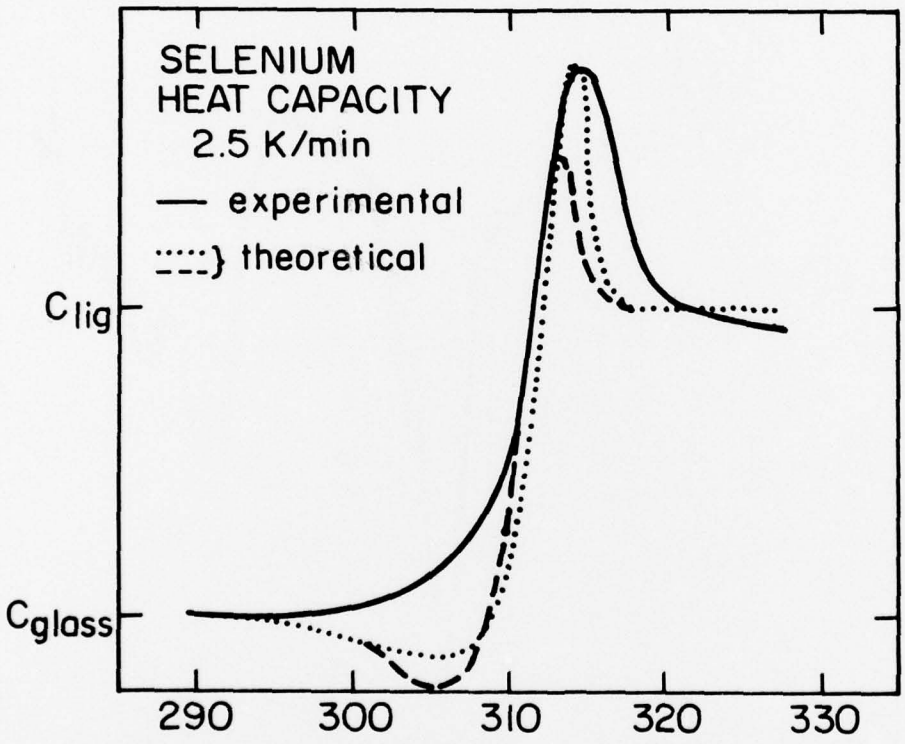

FIGURE 8: Selenium heat capacity recorded on a scanning calorimeter. The sample was cooled and then warmed at 2.5°K/min without any low temperature annealing. The dashed line is the heat capacity predicted by Eqs. (5) and (6) for those conditions and for $\tau(T)$ chosen so that T_g experimental and theoretical were within a few tenths of a degree for scans from 20 K/min to .3123 K/min. The dotted line is the heat capacity using a smaller configurational activation energy (55.6 kcal/mole) in the calculations. The amount of reduction was chosen so that the relaxation peak was the same height as the experimental trace.

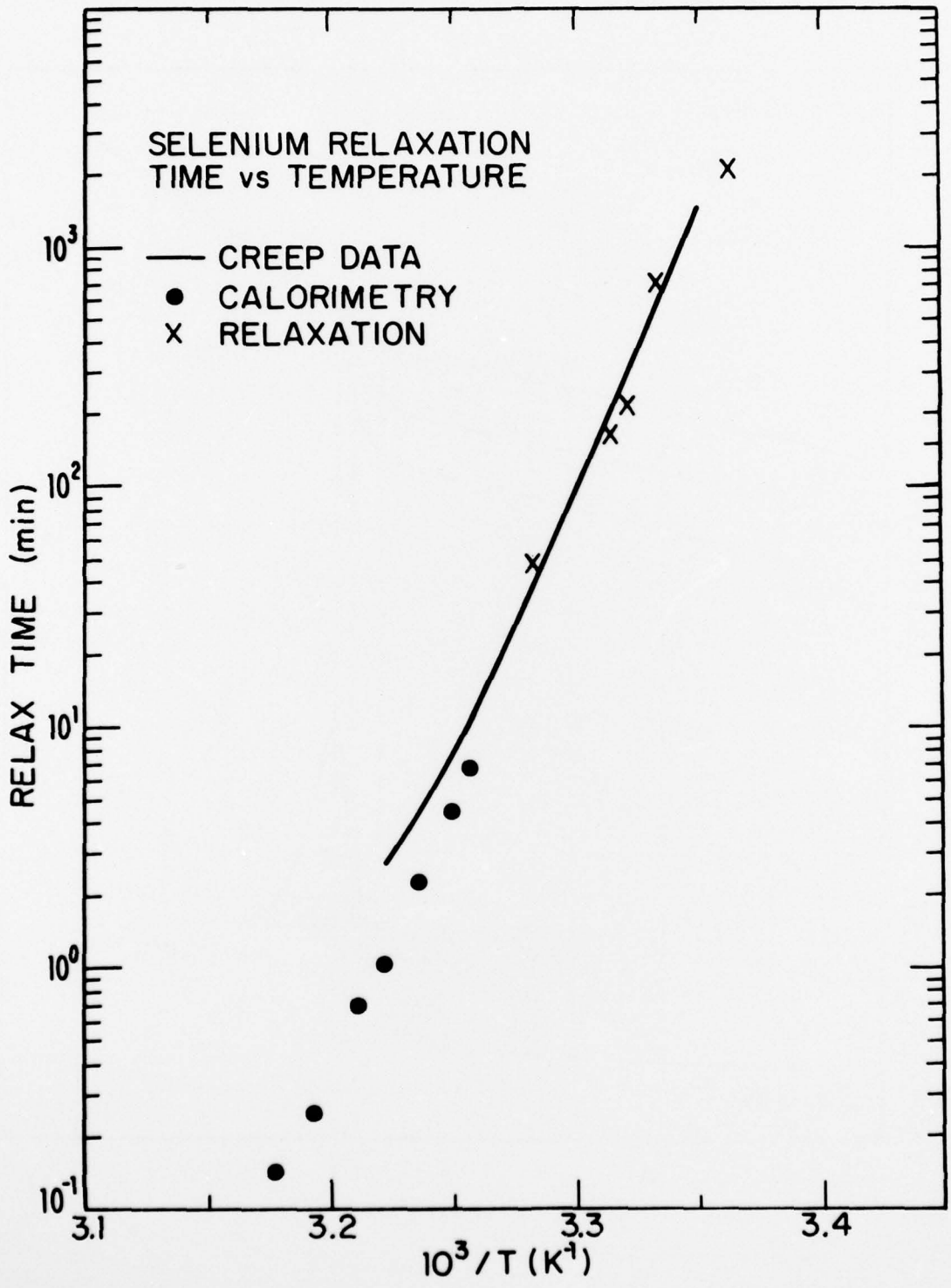

FIGURE 9: Selenium relaxation time vs. temperature calculated from three independent sources. The solid line is from viscosity data, and was gotten by combining the information in Figs. 2 and 6. The x's were from thermal relaxation measurements and the · are calculated from T_g vs. scan rate measurements.

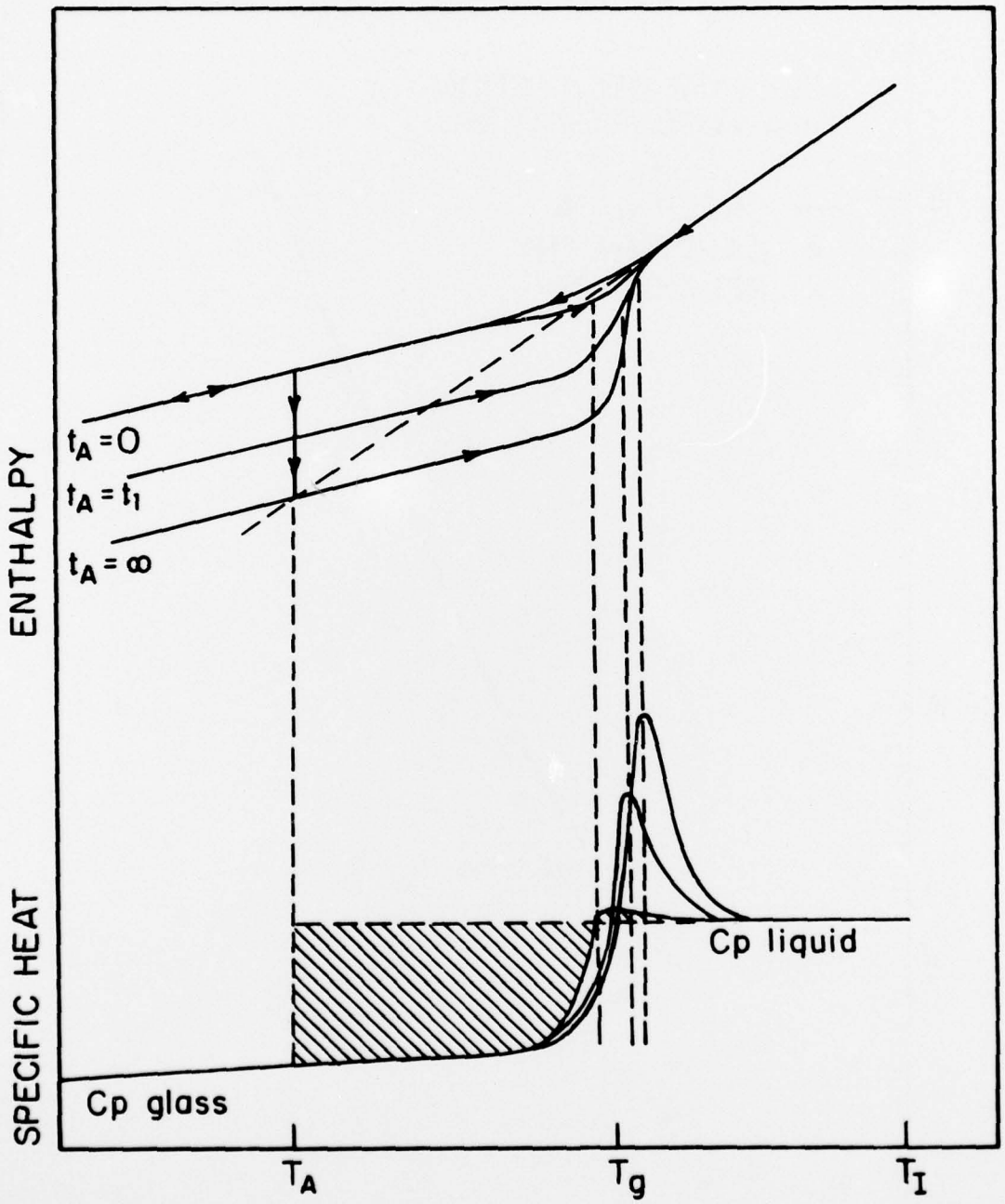

FIGURE 10: Enthalpy and heat capacity of a glass as it is cooled from an initial temperature T_I to T_A, annealed at T_A for varying lengths of time, t_A, and then warmed back to T_I at the same rate. The hatched area is the maximal energy one could anneal out by annealing at T_A.

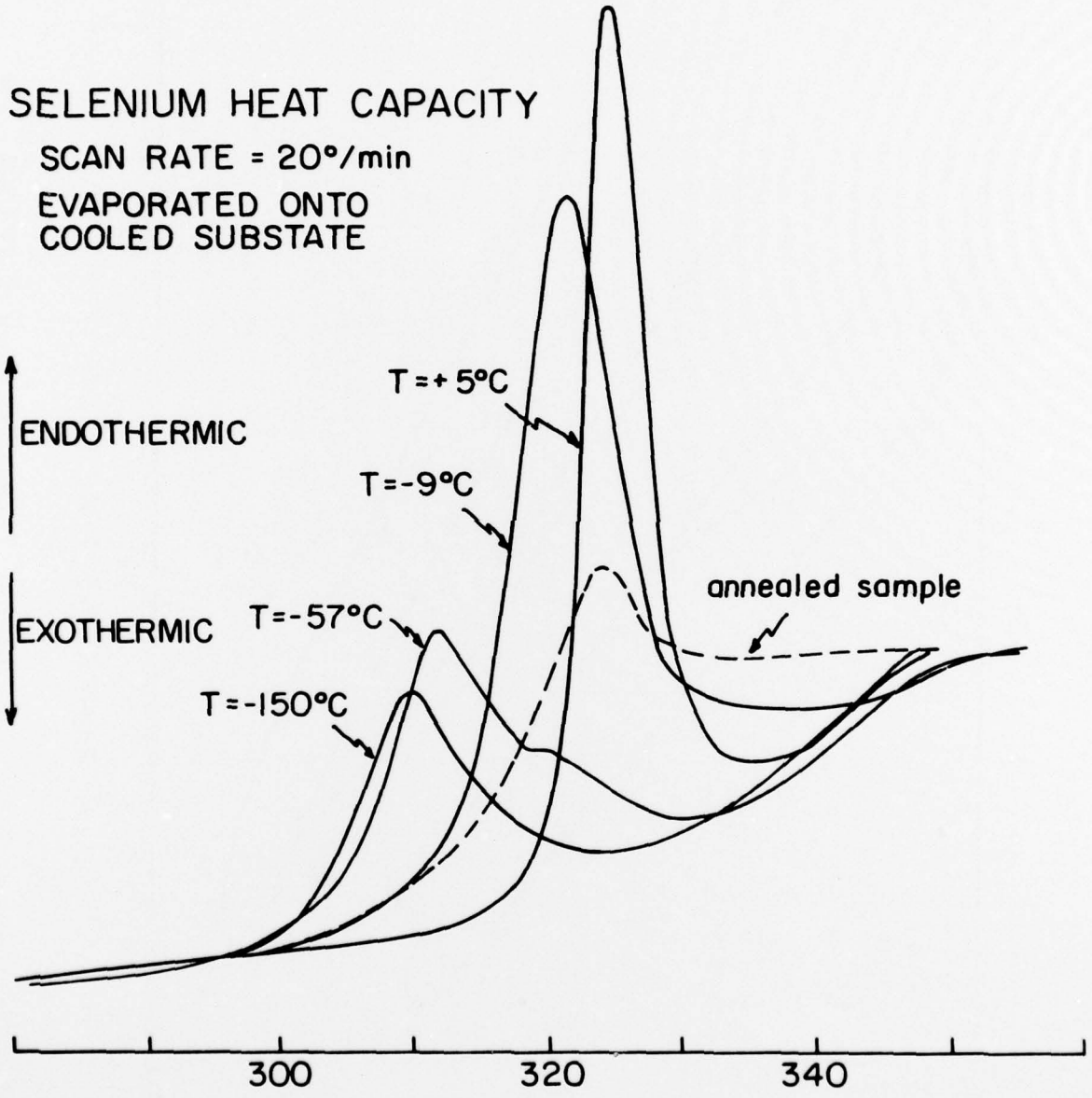

FIGURE 11: Fractional enthalpy relaxation of selenium vs. log annealing time at six different temperatures. The dotted curve is the form of the relaxation for a single activation energy. The dashed curve is the form of the thermal relaxation resulting from Eq. (1) for $T_A = 300°K$.

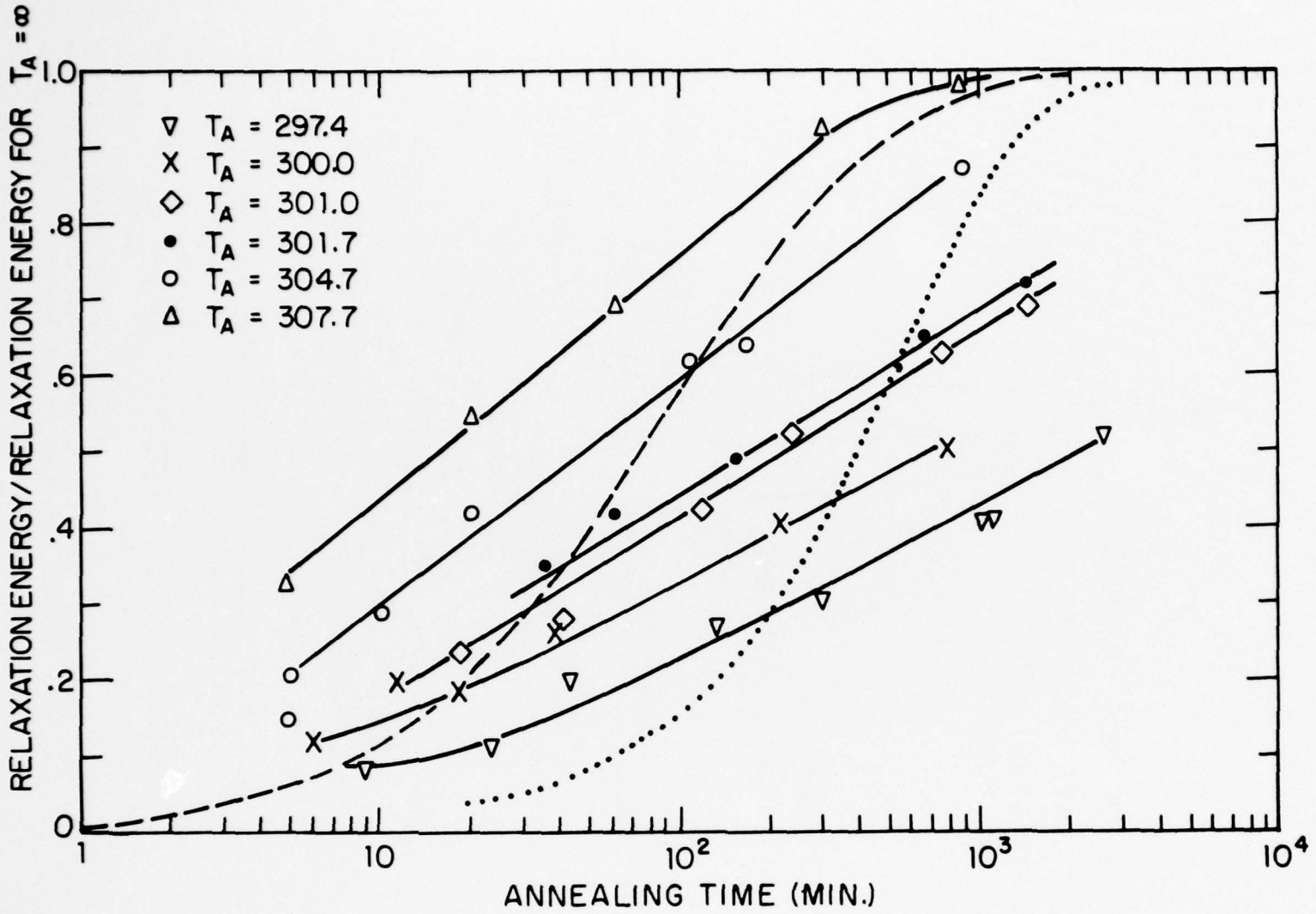

FIGURE 12: Selenium heat capacity vs. temperature at a scan rate of 20°K/min. The samples were evaporated onto a substrate cooled to temperature indicated in the figure.

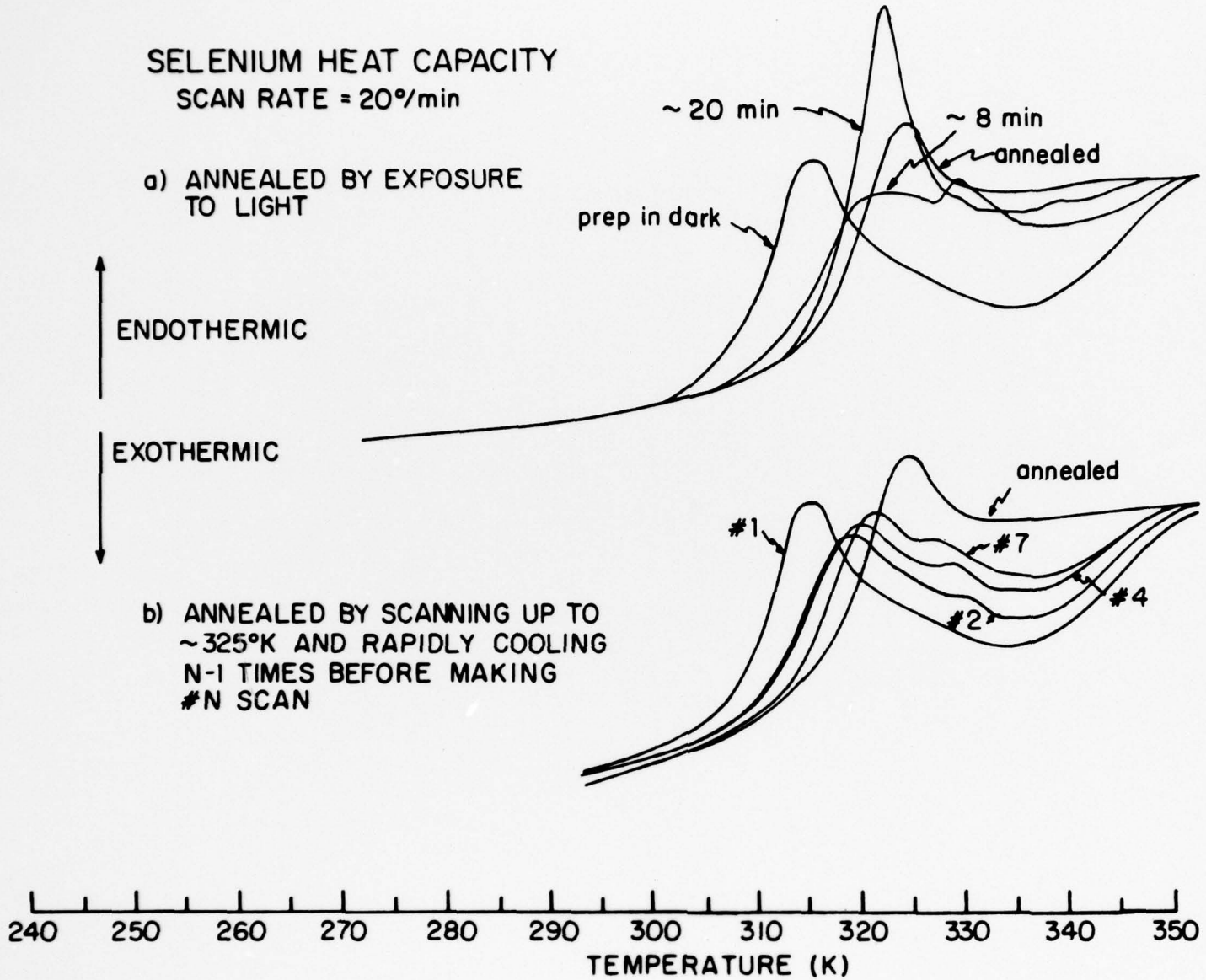

FIGURE 13: Selenium heat capacity vs. temperature at a scan rate of 20°K/min. The samples were evaporated onto a ~150°C substrate and then a) annealed at 0°C by exposure to a desk light whose intensity was 3.7 mW/cm^2, and b) by cycling the sample up to 322°K (n-1) times before making the #n scan to 350°C. After heating to 350°C, the heat capacities were identical to other annealed samples in all cases.

Defense Documentation Center
Cameron Station
Alexandria, Virginia 22314 (12)

Office of Naval Research
Department of the Navy
Attn: Code 471 (3)
Code 105 (6)
Code 470

Director
Office of Naval Research
Branch Office
495 Summer Street
Boston, Massachusetts 02210

Director
Office of Naval Research
Branch Office
536 South Clark Street
Chicago, Illinois 60605

Office of Naval Research
San Francisco Area Office
760 Market Street, Room 447
San Francisco, California 94102

Naval Research Laboratory
Washington, D.C. 20390
Attn: Code 6000
Code 6100
Code 6300
Code 6400
Code 2627 (6)

Attn: Mr. F.S. Williams
Naval Air Development Center
Code 302
Warminster, Pennsylvania 18974

Naval Air Propulsion Test Center
Trenton, New Jersey 08628
Attn: Library

Naval Weapons Laboratory
Dahlgren, Virginia 22448
Attn: Research Division

Naval Construction Batallion
Civil Engineering Laboratory
Port Hueneme, California 93043
Attn: Materials Division

Naval Electronics Laboratory Center
San Diego, California 92152
Attn: Electronic Materials Sciences Div.

Naval Missile Center
Materials Consultant
Code 3312-1
Point Mugu, California 93041

Commanding Officer
Naval Ordnance Laboratory
White Oak
Silver Spring, Maryland 20910
Attn: Library

Naval Ship R. and D. Center
Materials Department
Annapolis, Maryland 21402

Naval Undersea Center
San Diego, California 92132
Attn: Library

Naval Underwater System Center
Newport, Rhode Island 02840
Attn: Library

Naval Weapons Center
China Lake, California 93555
Attn: Library

Naval Postgraduate School
Monterey, California 93940
Attn: Materials Sciences Dept.

Naval Air Systems Command
Washington, D.C. 20360
Attn: Code 52031
Code 52032
Code 320

Naval Sea System Command
Washington, D.C. 20362
Attn: Code 035

Naval Facilities
Engineering Command
Alexandria, Virginia 22331
Attn: Code 03

Scientific Advisor
Commandant of the Marine Corps
Washington, D.C. 20380
Attn: Code AX

Naval Ship Engineering Center
Department of the Navy
Washington, D.C. 20360
Attn: Director, Materials Sciences

Army Research Office
Box CM, Duke Station
Durham, North Carolina 27706
Attn: Metallurgy and Ceramics Div.

Army Materials and Mechanics
Research Center
Watertown, Massachusetts 02172
Attn: Res. Programs Office (AMXMR-P)

Commanding General
Department of the Army
Frankford Arsenal
Philadelphia, Pennsylvania 19137
Attn: ORDBA-1320

Office of Scientific Research
Department of the Air Force
Washington, D.C. 20333
Attn: Solid State Div. (SRPS)

Aerospace Research Labs
Wright-Patterson AFB
Building 450
Dayton, Ohio 45433

Air Force Materials Lab (LA)
Wright-Patterson AFB
Dayton, Ohio 45433

NASA Headquarters
Washington, D.C. 20546
Attn: Code RRM

NASA
Lewis Research Center
21000 Brookpark Road
Cleveland, Ohio 44135
Attn: Library

National Bureau of Standards
Washington, D.C. 20234

Attn: Metallurgy Division
Inorganic Materials Division

Atomic Energy Commission
Washington, D.C. 20545
Attn: Metals and Materials Branch

Defense Metals and Ceramics
Information Center
Battelle Memorial Institute
505 King Avenue
Columbus, Ohio 43201

Director
Ordnance Research Laboratory
P.O. Box 30
State College, Pennsylvania 16801

Director Applied Physics Lab.
University of Washington
1013 Northeast Fortieth Street
Seattle, Washington 98105

Metals and Ceramics Division
Oak Ridge National Laboratory
P.O. Box X
Oak Ridge, Tennessee 37830

Los Alamos Scientific Lab.
P.O. Box 1663
Los Alamos, New Mexico 87544
Attn: Report Librarian

Argonne National Laboratory
Metallurgy Division
P.O. Box 229
Lemont, Illinois 60439

Brookhaven National Laboratory
Technical Information Division
Upton, Long Island
New York 11973
Attn: Research Library

Library
Building 50, Room 134
Lawrence Radiation Laboratory
Berkeley, California

Professor G.S. Ansell
Rensselaer Polytechnic Institute
Dept. of Metallurgical Engineering
Troy, New York 12181

Professor H.K. Birnbaum
University of Illinois
Department of Metallurty
Urbana, Illinois 61801

Dr. E.M. Breinan
United Aircraft Corporation
United Aircraft Research Lab.
East Hartford, Connecticut 06108

Professor H.D. Brody
University of Pittsburgh
School of Engineering
Pittsburgh, Pennsylvania 15213

Professor J.B. Cohen
Northwestern University
Dept. of Material Sciences
Evanston, Illinois 60201

Professor M. Cohen
Massachusetts Institute of Technology
Department of Metallurgy
Cambridge, Massachusetts 02139

Professor B.C. Giessen
Northeastern University
Department of Chemistry
Boston, Massachusetts 02115

Dr. G.T. Hahn
Battelle Memorial Institute
Department of Metallurgy
505 King Avenue
Columbus, Ohio 43201

Professor R.W. Heckel
Carnegie-Mellon University
Scienley Part
Pittsburgh, Pennsylvania 15213

Dr. David G. Howden
Battelle Memorial Institute
Columbus Laboratories
505 King Avenue
Columbus, Ohio 43201

Professor C.E. Jackson
Ohio State University
Dept. of Welding Engineering
190 West 19th Avenue
Columbus, Ohio 43210

Professor G. Judd
Rensselaer Polytechnic Institute
Dept. of Materials Engineering
Troy, New York 12181

Dr. C.S. Kortovich
TRW, Inc.
23555 Euclid Avenue
Cleveland, Ohio 44117

Professor D.A. Koss
Michigan Technological University
College of Engineering
Houghton, Michigan 49931

Professor A. Lawley
Drexel University
Dept. of Metallurgical Engineering
Philadelphia, Pennsylvania 19104

Dr. H. Margolin
Polytechnic Institute of New York
333 Jay Street
Brooklyn, New York 11201

Professor K. Masabuchi
Massachusetts Institute of Technology
Department of Ocean Engineering
Cambridge, Massachusetts 02139

Dr. G.H. Meier
University of Pittsburgh
Dept. of Metallurgical and Materials
Engineering
Pittsburgh, Pennsylvania 15213

Professor J.W. Morris, Jr.
University of California
College of Engineering
Berkeley, California 94720

Professor K. Ono
University of California
Materials Department
Los Angeles, California 90024

Professor W.F. Savage
Rensselaer Polytechnic Institute
School of Engineering
Troy, New York 12181

Dr. C. Shaw
Rockwell International Corp.
P.O. Box 1085
1049 Camino Dos Rios
Thousand Oaks, California 91360

Professor O.D. Sherby
Stanford University
Materials Sciences Dept.
Stanford, California 94300

Professor J. Shyne
Stanford University
Materials Sciences Department
Stanford, California 94300

Dr. W.A. Spitzig
U.S. Steel Corporation
Research Laboratory
Monroeville, Pennsylvania 15146

Dr. E.A. Starke, Jr.
Georgia Institute of Technology
School of Chemical Engineering
Atlanta, Georgia 30332

Professor N.S. Stoloff
Rensselaer Polytechnic Institute
School of Engineering
Troy, New York 12181

Dr. E.R. Thompson
United Aircraft Research Lab.
400 Main Street
East Hartford, Connecticut 06108

Professor David Turnbull
Harvard University
Division of Engineering and Applied
Physics
Cambridge, Massachusetts 02139

Dr. F.W. Wang
Naval Ordnance Laboratory
Physics Laboratory
White Oak
Silver Spring, Maryland 20910

Dr. J.C. Williams
Rockwell International
Science Center
P.O. Box 1085
Thousand Oaks, California 91360

Professor H.G.F. Wilsdorf
University of Virginia
Department of Materials Science
Charlottesville, Virginia 22903

Dr. M.A. Wright
University of Tennessee
Space Institute
Dept. of Metallurgical Engineering
Tullahoma, Tennessee 37388